第 24 卷 第 3 期
2005 年 5 月

岩 石 矿 物 学 杂 志
ACTA PETROLOGICA ET MINERALOGICA

Vol. 24, No. 3
May, 2005

内蒙乌拉山金矿床钾长石的矿物化学及有序度的分析

胡 萍[1,2], 赵令湖[1], 边秋娟[1]

(1. 中国地质大学, 湖北 武汉 430074; 2. Northeastern Illinois University, Chicago, IL 60625, USA)

摘 要: 采用电子探针显微分析(EMPA)和粉末 X 射线衍射(XRD)分析了采自乌拉山金矿床含金钾长石-石英脉、石英脉以及其他类型岩石中的 100 多个钾长石样品的化学成分和结果状态,并采用 R 和 Q 模式聚类分析、Spearman 等级相关分析方法对实验数据进行了统计分析。结果表明,含金矿脉、岩浆热液脉和蚀变花岗岩中的钾长石为中等到最大微斜长石,其特征为 K_2O 含量高,但相对而言,Na_2O、CaO 和 BaO 的含量低。其他岩石类型中的钾长石的化学成分和结果状态变化很大,可以从透长石、正长石到微斜长石,其特征为 K_2O 的含量相对较低,但 Na_2O、CaO 和 BaO 的含量相对较高。含金样品中的钾长石通常更富 K_2O,表明金的成矿作用与富钾的热液流体和碱质交代作用有关。乌拉山金矿床的成矿作用分为两个阶段,主要的含金钾长石-石英脉中的钾长石富 K_2O,形成温度为 307~379 ℃,平均为 353 ℃;第二阶段含金石英脉中的钾长石含 K_2O 较低,形成温度为 260~318 ℃,平均为 281 ℃。这些结果表明成矿流体与岩浆热液作用有关,流体朝温度降低、K_2O 含量降低的方向演化,K_2O 含量高的热液流体和 260~380 ℃的形成温度有利于金的成矿作用。

关键词: 乌拉山金矿床; 钾长石; 矿物化学; Al_Si 有序度; 统计分析

中图分类号: P578.968; P618.51 **文献标识码**: A **文章编号**: 1000-6524(2005)03-0221-10

Chemical and structural characteristics of K feldspars and their constrains to formation conditions of the Wulashan gold deposit, China

HU Ping[1,2], ZHAO Ling_hu[1], BIAN Qiu_juan[1]

(1. China University of Geosciences, Wuhan 430074, China; 2. Northeastern Illinois University, Chicago, IL 60625, USA)

Abstract: More than one hundred K feldspars were collected from gold_bearing Vein Ⅰ (K feldspar_quartz vein) and Vein Ⅱ (quartz vein) as well as various other rock types in the Wulashan gold deposit, China. Chemical compositions of K feldspars were analyzed using electron microprobe analysis (EMPA). The powder X_ray diffraction (XRD) patterns of K feldspars were collected using Cu Kα source. Au contents of the corresponding ore samples were analyzed by fire assay. Q_ and R_mode cluster analysis and Spearman rank correlation analysis of the experimental data were performed. The results indicate that K feldspars from gold_bearing veins, magmatic hydrothermal veins and altered wall rocks are intermediate to maximum microclines characterized by higher content of K_2O, lower contents of Na_2O, CaO and BaO, and relatively small variations in chemical compositions. K feldspars from other rock types are likely sanidine, orthoclase or microclines that show greater variations in chemical compositions and are characterized by lower content of K_2O but higher contents of Na_2O, CaO and BaO. K feldspars from auriferous samples are much richer in K_2O, indicating that gold mineralization might have been related to potassic hydrothermal fluids and intense K feldspar metasomatism. There exist two gold mineralization stages in the Wulashan deposit. K feldspars from the major K feldspar_quartz veins are characterized

收稿日期: 2004-09-14; **修订日期**: 2005-03-28

基金项目: 教育部科学技术研究基金资助项目(9549115)

作者简介: 胡 萍(1970-), 女, 汉族, 博士, 研究方向为矿物学。

by higher K_2O and higher formation temperatures of 307~ 379 ℃ with an average of 353 ℃. K feldspars from the quartz veins of the second stage are characterized by lower K_2O and lower formation temperatures of 260~ 318 ℃ with an average of 281 ℃. These results indicate that the mineralization fluids were associated with magmatic hydrothermal events and evolved toward lower temperatures and lower content of K_2O, but the hydrothermal fluids of higher K_2O and the temperatures of 260~ 380 ℃ may favor gold mineralization.

Key words: The Wulashan gold deposit; K feldspar, mineral chemistry; Al_Si degree of order; statistical analysis

1 Introduction

Geology and geochemistry of the Wulashan gold deposit have been extensively investigated and several ore genesis models have been proposed. They include descriptions of hydrothermal systems considered to be of magmatic (Nie & Bjørlykke, 1994; Hart *et al*., 2002; Miao *et al*., 2003), metamorphic (Gan *et al*., 1994), meteoric (Trumbull *et al*., 1996), and mixed magmatic_meteoric (Nie *et al*., 2002) water origins. In addition, ductile shear_controlled mineralization model (Zhang, 1989), triple (*i. e*., regional metamorphic – migmatization – shear deformation) mineralization model (Guan, 1993) and pegmatite_related mineralization model (Wu *et al*., 1995) are also proposed.

One unique feature of the Wulashan gold deposit is the intensive K feldspar metasomatism. Field studies show that K feldspar metasomatism is closely associated with the formation of gold mineralization in both space and time. Gold mineralization in the Wulashan gold deposit occurs in K feldspar – quartz or quartz veins. K feldspar also widely exists in all varieties of rock types in this area. However, the mineralogical study of K feldspars in this deposit has not been reported in detail so far. It is well known that chemical compositions and structural state of K feldspars are dependent on crystal_physical parameters and other external factors such as temperature, pressure, oxygen fugacity, availability of fluid phases, whole_rock composition, and coexisting mineral associations (Ribbe, 1983). Therefore, K feldspar is considered to be a useful monitor of the physicochemical environment in which it grows and a valuable indicator of the metallogenetic potential of the host rock (Plymate *et al*., 1992, Neves *et al*., 2001).

The purposes of this study are (i) to determine chemical compositions and structure state of K feldspars from gold_bearing veins and other rock types in the Wulashan gold deposit, (ii) to characterize or distinguish K feldspars from different ore or rock types using graphical methods and statistical analyses, (iii) to provide constrains to the formation conditions of the Wulashan gold deposit, based on the chemical and structural characteristics of K feldspars.

2 Geological setting

The Wulashan gold deposit is situated along the northwestern margin of the North China craton, and on the northern side of the Daqingshan – Wulashan fault belt (Zhang, 1989; Hu *et al*., 1990). The major host rocks are Archean high_grade metamorphic volcano_sedimentary rocks of the Wulashan Group, *e. g*., banded amphibolite, garnet_biotite_plagioclase gneiss, hornblende_plagioclase gneiss, sillimanite_biotite gneiss, and magnetite_plagioclase_orthopyroxene_clinopyroxene granulite (Shen *et al*., 1990). The Late Paleozoic Dahuabei granitoid batholite, lying just about 4 kilometers west to the Wulashan gold deposit, is the major intrusion in this area, which intruded the Archean Wulashan Group. In addition, there are also a number of granitoid stocks, pegmatite dikes, migmatite veins, K feldspar alterations and magmatic hydrothermal veins in this area (Zhang, 1991). Gold mineralization occurs in quartz_K feldspar and quartz veins with small amounts of base metal sulfides (pyrite, chalcopyrite and galena *etc*.). The mineralization ore veins are 200– 500 m (up to 3 000 m) long

in E_W or close to E_W direction, 1– 3 m (up to 10 m) wide, and 250– 400 m deep, and are spatially associated with the intrusive stocks, dikes and veins (Meng *et al.*, 2002). Alterations around the K feldspar_quartz and quartz veins consist mainly of K feldspathization, silicification, and less intensive pyritization, carbonatization, sericitization, and chloritization. The width of the alteration envelope ranges from 3 to 5 m (Zhang, 1991). K faldspathization and silicification are closely associated with gold mineralization. In fact, Au content of altered wall rocks is so high that these rocks constitute the third type of gold ores.

3 Samples and experiments

More than one hundred samples were collected from (1) regional metamorphic rocks (*e. g.*, biotite_plagioclase gneiss, biotite_muscovite_plagioclase gneiss, muscovite_plagioclase gneiss and feldspar_quartz gneiss), (2) migmatite, (3) granite, (4) altered granite, (5) pegmatite, (6) magmatic hydrothermal veins, (7) altered wall rock, (8) gold_bearing Vein Ⅰ (K feldspar_quartz veins), and (9) gold_bearing Vein Ⅱ (quartz veins) in the Wulashan gold deposit. The chemical compositions of K feldspars in thin sections were analyzed using JEOL model 733 electron microprobe operated at 15 kV and 10 nA. On_line data reduction and the matrix correction procedure of Bence and Albee (1968) were employed. A K feldspar sample of known compositions was employed for standardization. Counting times were optimized to provide the lowest possible counting_statistical errors and minimize the electron beam damage to the samples. For example, the counting time of 20 seconds for Na as the first element in each analysis was used to produce acceptable counting_statistic errors and to result in no measurable loss in Na X_ray intensity during the analysis. The analytical uncertainties based on counting statistics are estimated at the level of ~ 2% of the amount present (one standard deviation, 1σ) for major elements. Powder X_ray diffraction (XRD) patterns of different groups of K feldspars were recorded using Siemens XRD diffractometer with Cu Kα as a radiation source. In addition, Au contents of sixty_two ore samples from which K feldspars were separated were analyzed by fire assay.

4 Statistical analysis methods

Selection of the most appropriate statistic methods was based on the consideration whether the data distribution was normal (*i. e.* symmetrical, bell shaped curves) or was asymmetric or skewed in one way or another. The normality testing was firstly carried out on the compositional data of K feldspars. The outliers were not included in the statistical analysis. The cluster analysis was used in this study, because it is designed to perform classification by assigning observations to groups so that each group is more_or_less homogeneous and distinct from other groups (Davis, 1986). The cluster analysis does not require many of the assumptions that other statistical methods do, except for the heterogeneous data, and provides an easily understandable graphic display (dendrogram). It helps identify natural groupings for samples (Q_mode) or variables (R_mode) and, in turn, to reduce the numbers of groups for the samples or variables. Minitab program (version 14) was used to conduct cluster analysis. The ion numbers of elements in K feldspars from different ore and rock types or groups were used for Q_mode cluster analysis. All variables were standardized in order to avoid the influence of the magnitude of a particular variable, and the Cosine theta similarity coefficient was used. Meanwhile, all K feldspars from gold_bearing ore samples were divided into two groups: auriferous samples (> 0. 2 g/t Au) and barren samples (< 0. 2 g/t Au). The R_mode cluster analysis were performed on the datasets of K feldspars from (i) auriferous samples (N= 25), (ii) barren samples (N= 37), and (iii) all samples (N = 25+ 37). The absolute correlation coefficients were used as the similarity measures.

In addition, the Spearman rank correlation coefficient analysis (Rs) was utilized. This non_parametric statistical analysis is suitable for the comparison of

data with large fluctuations. The Rs is related to the number (N) of samples and describes the probability (p) that the correlation is not significant. The dataset for Spearman rank correlation coefficient analysis was the same as that for R_mode analysis, and NCSS 2004 statistical software was used to calculate the Spearman rank correlation coefficients.

5 Results

The ion number of each element in K feldspar is calculated based on chemical compositions analyzed by EMPA and 8 oxygen atoms per formula unit, and the results of representative K feldspars are given in Table 1. The average end_member compositions of K feldspars from different rock or ore types are given in Table 2. In general, the content of $CaAl_2Si_2O_8$(An) in K feldspars from the Wulashan gold deposit is 0–1.7 mol% with an average of 0.5±0.6 mol%. The contents of $NaAlSi_3O_8$(Ab) and $KAlSi_3O_8$(Or) in K feldspars from regional metamorphic gneiss, migmatites, granite and pegmatites changed in a greater range, with Ab from 1.3–37.7 mol%, and Or from 62.1–98.6 mol%. However, in K feldspars from magmatic hydrothermal veins, and gold_bearing veins Ⅰ and Ⅱ, the content of Ab is < 6 mol% and that of Or is > 94 mol%.

The Al_Si degrees of order of K feldspars were calculated based on the $2\theta_{060}$ and $2\theta_{113}$ in powder XRD patterns (Hovis, 1986) (Table 1), and the average Al_Si degrees of order of K feldspars from different rock types are given in Table 2. The Al_Si degree of order (Z) of K feldspars from regional metamorphic gneiss, migmatites, granites, altered granites and altered wall rocks vary from 0.27 to 0.95, corresponding to the K feldspars from sanidine, orthoclase, and intermediate to maximum microclines. The alteration of granite resulted in the increase of Al_Si degree of order and the transition of K feldspars from orthoclase to microclines. In contrast, the K feldspars from pegmatites, magmatic hydrothermal veins, gold_bearing veins Ⅰ and Ⅱ are intermediate to maximum microclines,

Table 1 Chemical compositions and Al_Si degree of order of representative K feldspars

		Au(g/T)	Ion number per K feldspar molecule												Z
			K	Na	Ca	Ba	Mg	Fe	Mn	Ni	Cr	Ti	Al	Si	
RMR	309	0.018	0.898	0.103	0.011	0	0.011	0.002	0	0.002	0.002	0.006	0.970	2.998	0.89
	312	0	0.929	0.076	0.010	0	0	0.003	0	0	0	0.005	0.983	3.000	0.93
Migmatite	901_3	0.017	0.632	0.384	0.002	0	0	0	0.002	0.007	0.024	0.007	0.951	2.964	0.89
	384	0.065	0.956	0.034	0.002	0.002	0	0	0	0	0	0	0.977	3.017	0.90
	388	0.021	0.962	0.042	0	0.012	0	0.002	0	0.004	0.001	0	0.976	3.003	0.92
Granite	9A_1	0.0005	0.586	0.258	0.002	0	0	0.003	0	0	0	0.009	0.969	3.000	0.62
	306	0	0.803	0.107	0.006	0.003	0.008	0.002	0	0.010	0.001	0	0.976	3.000	0.68
	338	0	0.890	0.108	0.007	0.010	0.006	0.008	0	0.001	0.002	0.002	0.973	2.999	0.70
Altered granite	3111	0.065	0.857	0.097	0.002	0.018	0	0.003	0	0	0.002	0	0.965	3.000	0.86
	326	0.034	0.988	0.043	0.006	0.018	0	0.002	0	0.008	0	0	0.934	2.972	0.86
	342	0	0.940	0.077	0	0.004	0	0.001	0.003	0.014	0.001	0.002	0.958	2.991	0.71
Pegmatite	366	0.10	0.938	0.064	0	0.003	0	0.006	0	0.002	0	0.001	0.976	3.009	0.93
	382	0.34	0.915	0.040	0	0.010	0	0.001	0	0	0.004	0	0.979	3.019	0.95
MHV	4151	0.02	0.910	0.051	0	0	0	0.013	0	0.004	0.002	0.006	0.971	3.014	0.92
Gold_bearing vein Ⅰ	354_1	0.56	0.928	0.071	0.005	0.014	0	0.002	0	0.003	0	0	0.978	2.991	0.92
	317	40.00	0.902	0.039	0.008	0	0.010	0.005	0.002	0	0	0.002	0.971	3.022	0.84
	C139	5.41	0.901	0.031	0	0.002	0	0.001	0	0	0.006	0	0.929	3.000	0.89
	331	0.255	1.005	0.050	0	0	0	0.002	0.001	0.003	0	0	0.939	2.970	0.98
Gold_bearing vein Ⅱ	C181	20.05	0.999	0.007	0.002	0	0	0	0.006	0.002	0	0.009	0.942	3.000	0.81
	334	1.50	0.934	0.031	0.006	0	0.006	0.012	0	0	0.002	0.001	0.974	3.014	0.93
	336	5.20	0.941	0.025	0.011	0.002	0.003	0	0	0	0.003	0.003	0.964	3.022	0.89
	367	0.26	0.910	0.023	0.006	0.011	0	0.002	0	0	0.015	0	0.983	3.009	0.92

RMR—Regional metamorphic rocks; MHV—Magmatic hydrothermal veins.

Table 2　The averages of Al_Si degree of order (Z) and end_member compositions (Or, Ab and An) in K feldspars from different geological bodies

Rock types	Al_Si degree of order (Z)	End_member compositions		
		Or	Ab	An
Regional metamorphic rocks	0.72	92.5	7.0	0.5
Migmatite	0.89	87.5	12.2	0.3
Granite	0.76	83.8	15.8	0.5
Altered granite	0.85	93.6	6.2	0.2
Pegmatite	0.93	88.9	11.0	0.2
Magmatic hydrothermal veins	0.87	95.2	4.7	0.1
Altered wall rock	0.76	96.4	3.4	0.2
Gold_bearing veins	0.89	95.5	4.3	0.3

with Z from 0.81 to 0.98. The Al_Si degree of order for the K feldspars from gold_bearing veins varies even in a more narrow range. The end member compositions and Al_Si degree of order of K feldspars in Table 2 indicates the similarity of K feldspars from gold_bearing veins and magmatic hydrothermal veins.

5.1　Box plot of K/(K+ Na)

Box plot of the ion number ratio, K/(K + Na), in K feldspars of different rock and ore types or groups is shown in Fig. 1, where the outlier data points are marked by asterisks, and three measures, 15^{th}, 50^{th}, and 85^{th} percentiles, indicate the variation range and central tendency of K/(K+ Na) ratio. This plot expresses the variability of the parameter, K/(K+ Na), in the range of 15^{th}– 85^{th} percentiles and in the median or 50th percentile that are directly comparable for different groups, regardless of the data distribution patterns. The K/(K+ Na) ratio of K feldspars from magmatic hydrothermal vein (No. 6), altered wall rock (No. 7), gold_bearing veins Ⅰ and Ⅱ (No. 8, 9) changes in a narrow range and the medians are above the reference line that is the median data of K feldspar from the magmatic hydrothermal vein. The K feldspars from gold_bearing veins and magmatic hydrothermal veins are characterized by relatively higher content of K and lower content of Na. However, the K/(K+ Na) ratio for K feldspars from the other rock types changes in greater ranges, even with outlier data points, and the medians are below the same reference line. These results enable us to differentiate different types of rock or ore samples.

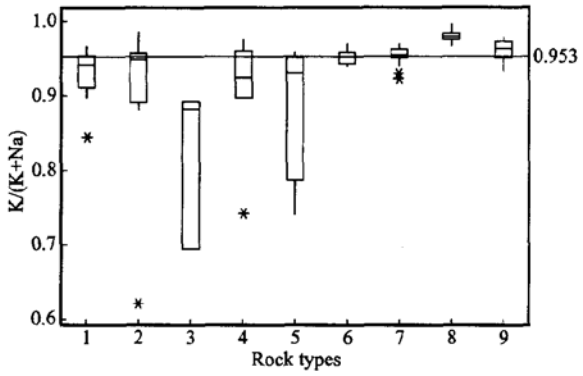

Fig. 1　Variation of K/(K + Na) in K feldspars from different groups or geological bodies

1—Regional metamorphic gneiss; 2—Migmatite; 3—Granite; 4—Altered granite; 5—Pegmatite; 6—Magmatic hydrothermal veins; 7—Altered wall rock; 8—Gold_bearing veins Ⅰ; 9—Gold_bearing veins Ⅱ

5.2　Scatter plot of (Ca+ Na)/K versus the ion number of Ba

The scatter plot of the ion number ratio, (Ca + Na)/K, versus the ion number of Ba in K feldspars from different rock types or groups is shown in Fig. 2. Almost all data points of K feldspars from magmatic hydrothermal vein (No. 6) and mineralized ore veins (No. 8 and 9) fall in the rectangular area defined by Ba < 0.011 and (Ca+ Na)/K< 0.07. These results indicate that the K feldspars from gold_bearing veins and hydrothermal veins have higher content of K but relatively lower content of Na, Ca and Ba. In contrast, the data points of K feldspars from the other rock types are more scattering in distribution and fall outside the rectangular area. Several K feldspars from migmatites, granite, altered granite and pegmatite even have the (Ca+ Na)/K> 0.2. These results indicate that chemical compositions of K feldspars from these rock types vary in greater ranges and are characterized by lower content of K but relatively higher contents of Na, Ca and Ba. Furthermore, the scattering plot of the chemical compositions of K feldspars can not only help distinguish the K feldspars from the gold_bearing veins from the other rock types, but also indicate that formation conditions of magmatic hydrothermal veins and mineralized lodes may be more similar to each other than those of the other rock types.

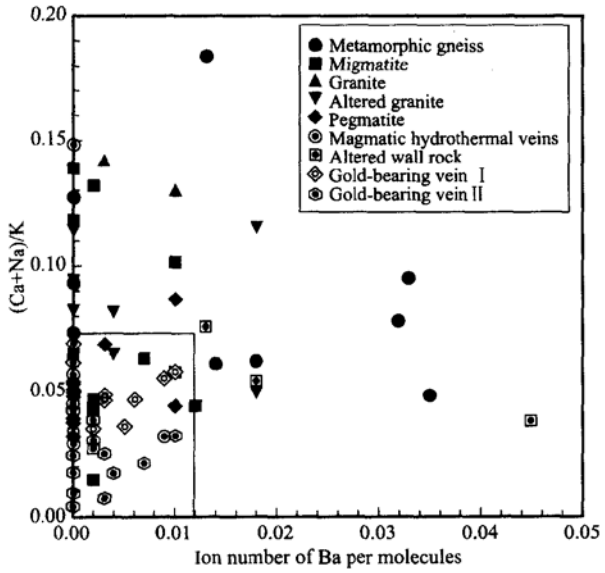

Fig. 2 Variation of Ba (ion number per molecule) against the ratio of (Ca+ Na)/K in K feldspars

5.3 Q_mode cluster analysis

The dendrogram of the Q_mode cluster analysis is shown in Fig. 3. It indicates that the four groups of samples are recognized at the level of clustering as follows:

Group 1: Gneiss and altered granite

Group 2: Magmatic hydrothermal vein, gold_bearing veins, and altered wall rock

Group 3: Migmatite and pegmatite

Group 4: Granite

It is again shown that K feldspars from magmatic hydrothermal veins, altered wall rock and gold_bearing veins are more similar to each other, rather than K feldspars from gneiss, migmatite, granite and pegmatite.

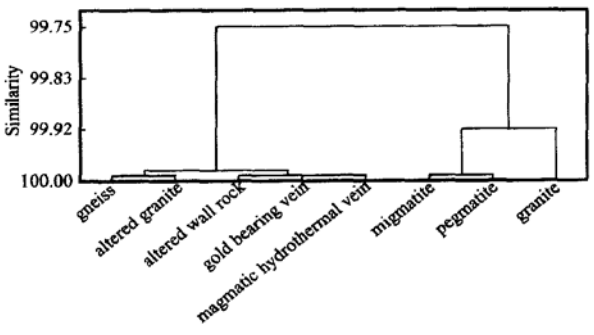

Fig. 3 Dendrogram of the Q_mode cluster analysis

5.4 R_mode cluster analysis

The dendrograms of the R_mode cluster analyses for K feldspars from auriferous and barren samples are shown in Fig. 4 and 5, respectively. The dendrogram from R_mode cluster analysis of all samples is not shown, because it is similar to that of barren samples. The dendrogram from the R_mode analysis shows that the element pair Na- Fe has significant correlations for K feldspars from auriferous samples and could be used as an indicator of gold mineralization. The elemental groupings of Si- Al with Ba, and Mn- Ti are common for K feldspars from either auriferous, barren or all samples.

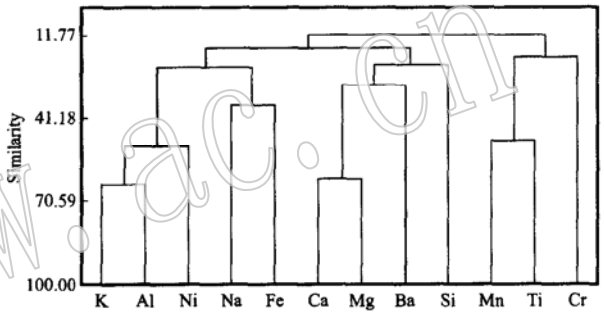

Fig. 4 Dendrogram of R_mode cluster analysis for K feldspars from auriferous samples

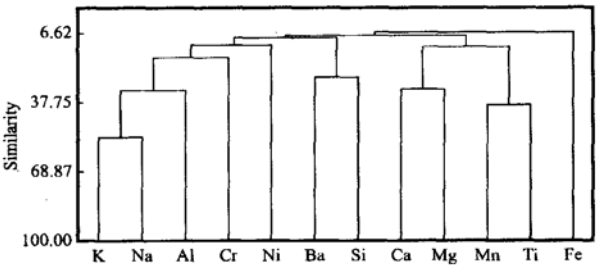

Fig. 5 Dendrogram of R_mode cluster analysis for K feldspars from barren samples

5.5 Spearman rank correlation coefficient analysis

The elemental mean and other statistical parameters (standard deviation, standard error, minimum, maximum, median, skewness and kurtosis) of K feldspars from auriferious and barren samples are summarized in Table 3. The mean of each element in K feldspars from auriferous samples was divided by the mean of the same element in K feldspars from barren

samples. The resulting ratio indicates the relative enrichment or depletion of each element between two groups of K feldspars. In general, the K feldspars from auriferous samples have higher K and Cr but lower Na, Ba, Mg, Mn, Ti and Ni than the barren K feldspars. The means of Ca, Fe, Al and Si are similar between the two groups of samples.

Spearman rank correlation coefficient (Rs) was computed to investigate the relationships between Au content and element compositions of K feldspars. The most positive correlations between the Au content and specific elements among the auriferous, barren and all K feldspar samples are summarized in Table 4. It indicates that Si and Ba in K feldspars seem to be an indicator for auriferous and barren samples. For all K feldspars as a dataset, K is a characteristic element, which again indicates that high content of K_2O characterizes the K feldspars from the Wulashan gold lodes.

Table 3　The means and related statistical parameters of chemical compositions of K feldspars from auriferous and barren samples

	Au(g/T)	Ion number per molecule											
		K	Na	Ca	Ba	Mg	Fe	Mn	Ni	Cr	Ti	Al	Si
K feldspar (N = 37) from barren samples													
Mean	0.039	0.894	0.071	0.003	0.006	0.002	0.005	0.002	0.002	0.002	0.004	0.973	2.994
Std. dev.	0.052	0.096	0.047	0.004	0.010	0.003	0.011	0.002	0.003	0.002	0.004	0.028	0.022
Std. error	0.008	0.016	0.008	0.001	0.001	0.000	0.000	0.000	0.000	0.000	0.001	0.005	0.004
Min	0.000	0.567	0.016	0.000	0.000	0.000	0.002	0.000	0.000	0.000	0.000	0.914	2.936
Median	0.020	0.925	0.064	0.002	0.001	0.000	0.071	0.010	0.001	0.001	0.002	0.976	2.998
Max	0.192	1.018	0.258	0.017	0.035	0.011	0.002	0.000	0.014	0.007	0.017	1.043	3.041
Skewness	1.89	2.04	2.29	1.60	1.84	2.01	5.50	1.63	1.89	1.03	1.37	0.27	- 0.53
Kurtosis	3.01	4.39	7.01	2.42	2.60	2.82	32.10	2.60	4.87	- 0.04	1.61	0.64	0.47
K feldspar (N = 25) from auriferous samples													
Mean	12.50	0.923	0.030	0.003	0.005	0.001	0.005	0.001	0.001	0.004	0.002	0.979	2.994
Std. dev.	21.65	0.076	0.013	0.004	0.010	0.002	0.007	0.001	0.002	0.005	0.002	0.031	0.033
Std. error	4.33	0.015	0.003	0.001	0.002	0.000	0.001	0.000	0.001	0.000	0.000	0.006	0.007
Min	0.210	0.732	0.007	0.000	0.000	0.000	0.000	0.000	0.000	0.000	0.000	0.926	2.884
Median	3.11	0.934	0.030	0.002	0.002	0.000	0.002	0.000	0.000	0.002	0.001	0.975	2.998
Max	81.17	1.018	0.050	0.014	0.045	0.007	0.034	0.006	0.006	0.022	0.009	1.054	3.067
Skewness	2.26	- 1.02	- 0.08	1.56	2.93	1.37	2.94	2.64	1.26	2.41			
Kurtosis	4.47	0.61	- 1.03	2.05	9.59	0.76	10.62	7.51	0.11	6.66			
Ratio of mean*		1.032	0.423	1.000	0.833	0.500	1.000	0.500	0.500	2.000	0.500	1.006	1.000

* $Ratio\ of\ mean = \frac{Mean\ of\ an\ element\ in\ K\ feldspar\ from\ auriferous\ samle}{mean\ of\ the\ same\ element\ in\ K\ feldspar\ from\ barren\ sample}$

Table 4　Significant Spearman rank correlation coefficients between the chemical compositions and the Au contents of the whole rock or ore samples

Sample set	N	Element	Spearman rank coefficients (Rs)	P value
Total	62	K	0.217	0.066
Auriferous	25	Si	0.270	0.200
Barren	37	Ba	0.288	0.084

The statistically significant element pairs were determined for auriferous, barren and all samples. The cut_off values used to define the significance were high (*i. e.* Rs> 0.31 for p= 0.056), which is related to the number of samples (N). Like the cluster analysis, the following elements, Ca, Mg, Ba, Al and Si, and the elemental groupings of Si- Al with Ba, and Mn - Ti, are common to the K feldspars from both auriferous and barren samples. However, the elemental pairs, K- Ni; Ca- Si, Mg; Fe- Mg; Al- Ba, statistically characterize K feldspars from auriferous samples; the elemental pairs, K- Ba, Al; Ti - Ca, Mg, Mn; Ba- Cr; Fe- Al, statistically characterize the K feldspars from barren samples.

6 Discussion and conclusions

6.1 K feldspars from gold_bearing veins and other rock types

K feldspars from gold_bearing veins and magmatic hydrothermal veins are very similar in chemical compositions and Al_Si degree of order. These K feldspars are characterized by higher contents of K, lower contents of Na, Ca, Ba, and relatively insignificant variations in chemical compositions. The Al_Si degree of order of K feldspars ranges from 0.81 to 0.98, indicating that K feldspars are intermediate to maximum microclines and the formation temperatures should be lower than 450℃ (Ribbe, 1983). The results also indicate that the gold_bearing veins and magmatic hydrothermal veins may be closely associated in genesis and the gold mineralization in the Wulashan gold deposit is, at least partially, related to the magmatic hydrothermal fluids of high K_2O, SiO_2, and Au. However, chemical characteristics of K feldspars cannot clearly indicate which intrusions or magmatic events in this area are more likely related to the gold mineralization, although the Late Paleozoic Dahuabei granitoid batholite appears to be one logical source of hydrothermal fluid for the Wulashan gold mineralization. These results are in agreement with the previous studies of isotopes and fluid inclusions (Gan *et al*., 1994, Nie *et al*., 2002, Hart *et al*., 2002, Miao *et al*., 2003). These authors found that there are two distinct major gold mineralization episodes in the Wulashan gold deposit, a Late Paleozoic (352 Ma) gold mineralization and a Late Mesozic (132 Ma) gold mineralization (Miao *et al*., 2003). The first mineralization episode is coeval with the emplacement of the Dahuabei granite batholith (Nie *et al*., 2002, Miao *et al*., 2003). However, Gan *et al*. (1994) indicate that there are significant differences in the characteristics of fluid inclusions between the gold ore veins and the Dahuabei granioid batholith. Therefore, gold mineralization at the Wulashan gold deposit may be not restricted to a single mineralizing event and the hydrothermal fluids may be not restricted to a single source, which requires more understanding of the complex tectonic, magmatic and thermal history integrated with geological and geochronological studies (Hart *et al*., 2002).

In addition, most K feldspars from altered wall rocks are also similar to those from gold_bearing veins and magmatic hydrothermal veins, as evidenced by the cluster analysis which indicates that K feldspars from the three rock types are classified into the same group. However, the chemical compositions and Al_Si degree of order of K feldspars from the altered wall rocks change in greater ranges. These results indicate that most K feldspars in the altered wall rocks were formed or re_crystalized while the mineralization fluids were in equilibrium with the wall rocks. During the alteration processes of K feldspathization, silicification, pyritization, carbonatization and sericitization, K_2O, SiO_2, CO_2, S and Au in the mineralization fluids were brought into the wall rocks, while Na_2O, FeO, MgO, TiO_2, Al_2O_3 and H_2O into the fluids. As a result, intense Au mineralization occurred in the altered wall rocks with a large amount of K feldspars of high K_2O.

There are two distinct mineralization stages in the Wulashan gold deposit: the gold_bearing veins (K feldspar_quartz veins) and gold_bearing veins (quartz veins). The K feldspar_quartz veins resulting from the major gold mineralization stage are characterized by high potassic fluid, intense feldspathization, large amounts of K feldspars, and high content of K in K feldspar. The formation temperatures of the gold_bearing veins Ⅰ are estimated to be 307~379℃, with an average of 353℃ (Hu *et al*., 2004). The mineralization fluids were evolved to be less potassic and more silicic at the second stage gold mineralization and, as a result, the quartz veins were formed with less intense feldspathization, more intense silicification and less K feldspars in mineralized lodes and lower content of K in K feldspars. The mineralization temperatures for the gold_bearing quartz veins are estimated to be 260~318℃, with an average of 281℃ (Hu *et al*., 2004). These constrains on the formation conditions of the Wulashan gold deposit from the

chemical compositions and Al_Si degree of order of K feldspars are in agreement with the field observations and other fluid inclusion studies (Gan *et al.*, 1994, Wu *et al.*, 1995).

Chemical compositions and Al_Si degree of order of K feldspars from regional metamorphic gneiss, migmatites, granite and pegmatites are different than those of K feldspars from gold_bearing veins in two aspects. First, these K feldspars have relatively higher contents of Na, Ca, and Ba but lower content of K. Second, chemical compositions and Al_Si degree of order change in greater ranges. The formation temperatures of K feldspars also vary greatly even for K feldspars from the same rock types (Hu *et al.*, 2004). For example, in gneiss and migmatitites, some K feldspars have high content of Na and low Al_Si degree of order to 0.27, corresponding to sanidine or orthoclase. The formation temperatures of some K feldspars can be 700 – 800 ℃. However, most K feldspars from these rock types are intermediate to maximum microclines. The results suggest that K feldspars from these rock types may have experienced complex magmatic and thermal processes since they were formed, and therefore, K feldspars must have achieved re_equilibration. In fact, the alteration of granite might have resulted in the transformation of K feldspars from orthoclase to microcline with higher content of K and greater Al_Si degree of order.

6.2 K feldspars from auriferous and barren samples

The average contents of Ca, Fe, Al and Si are similar for K feldspars from auriferous and barren samples. However, K feldspars from auriferous samples are characterized by higher contents of K and Cr, whereas K feldspars from barren samples by higher contents of Na, Ba, Mg, Mn, Ni and Ti. The elemental groupings of Si– Al with Ba, and Mn– Ti are common to the K feldspars from both auriferous and barren samples. However, K feldspars from auriferous samples are statistically characterized by elemental pairs of K– Ni; Ca– Si, Mg; Fe– Mg; and Al– Ba, whereas K feldspars from barren samples by elemental pairs of K– Ba, Al; Ti– Ca, Mg, Mn; Ba– Cr; and Fe– Al. There is a strong correlation between K_2O in K feldspars and Au content of all ore samples. These results suggest that the enrichment of gold should be related to the high content of K_2O in hydrothermal fluids or intense potassic metasomatism, and the content of K_2O in K feldspars may be used as an indicator of gold mineralization.

The K feldspars of auriferous samples are characterized by low contents of element pairs Na– Fe and Fe– Mg. It might indicate the leaching of Fe during potassic alteration, resulting in the formation of pyrite, hematite and magnetite, which is in good agreement with field observations in the Wulashan gold deposit. The enrichment of gold ores is proportionally related to the amount of pyrite in the gold ores, and more hematite and magnetite are observed in the major K feldspar_quartz veins of this deposit. The K feldspars from barren samples are statistically characterized by relatively higher content of Ba and many other transition elements, and the elemental Ba– Cr and Ti– Mn. These results indicate that the high contents of Ba and other transition elements in K feldspars may be indicators of poor gold mineralization, and the high contents of these elements in hydrothermal fluids may not favor the gold mineralization, which is in agreement with a previous study (Xue *et al.*, 2000).

References

BENCE, A. E. & ALBEE, A. L. 1968. Empirical correction factors for electron microanalysis of silicates and oxides. *J. Geol.*, 76: 382~ 403.

DAVIS J C. 1986. Statistics and Data Analysis in Geology (2nd ed.). Wiley, New York.

GAN, S.F., QIU, Y.M., YANG, H.Y. & VAN REENEN, D.D. 1994. The Hadamengoumine: a typical gold deposit in the Archean granulite facies terrane of the North China craton. *Int. Geol Rev.*, 36: 850~ 866.

GUAN, L.X. 1993. Ore_forming process of the Wulashan gold deposit, Inner Mongolia. *J. Gold Geosci.*, 3: 1~ 5 (in Chinese).

FENG Z X. & LI H Y. 2002. Analysis on geological character and controlling metalogenic of the ore bell of Bayanwula mountain in Azhuoqi, Inner Mongolia. *Mineral. Res. Geol.*, 16 (1): 9~ 12 (in Chinese).

HART C J R, GOLDFARB R J & QIU Y M. 2002. Gold deposits of the northern margin of the North China Craton: multiple late Paleozoic- Mesozoic mineralizing events. *Mineral. Deposita*, 37: 326~ 351.

HOVIS, G.L. 1986. Behavior of K feldspars: crystallographic properties and characterization of composition and Al_Si distribution. *Am. Mineral.*, 71: 869~ 890.

HU B Q, Chang Z Y. & Zhang W Z. 1990. Basic geologic features of Yinshan large_scale nappe structure and its relation to regional metallogeny of gold mineralization. *J. Inner Mongolia Geol.*, 1: 1~ 7 (in Chinese).

HU Ping, ZHAO Linghu and BIAN Qiujuan. 2004. Formation temperatures of alkali feldspars from the Wulashan gold deposit: an estimate by two_feldspar thermometry. *Acta Petrologica et mineralogica*, 23(4): 327~ 336 (in Chinese with English abstract).

LIANG, H.J. & ZHAO, C.R. 1999. Metallogenic condition and ore_control factor of hadamengou gold deposit, Inner Mongolia. *Gold Geol.*, 5 (2): 42~ 46 (in Chinese).

MENG W, CHEN X W & LI M W. 2002. Study on metallogenic epoch and metallogenic stages of the Hadamengou gold deposit, Inner Mongolia. *Gold Geol.*, 8(4): 13~ 17 (in Chinese).

MIAO L C, QIU Y M, MCNAUGHTON, N., FAN, W. M., GROVES, D. L. & ZHAI M G. 2003. SHRIMP U_Pb zircon ages of granitoids in the Wulashan gold deposit, Inner Mongolia, China: timing pf mineralization and tectonic implications. *Int. Geol Rev.*, 45: 541~ 562.

NEVES L. P. F, PEREIRA, A. J. S. C. & GODINHO, M. M. 2001. The role of cooling rate on the Al_Si order of K_feldspar in the Hercynian Tabua granite, Central Portugal. *Can. Mineral.*, 39: 85~ 92.

NIE F J. & BJøRLYKKE, N. 1994. Lead and surfur isotope studies of the Wulashan quartz_K feldspar and quart vein gold deposit, Southwestern Inner Mongolia, People's Republic of China. *Econ. Geol.*, 89: 1 289~ 1 305.

NIE F J, JIANG S H, SU X X. & WANG X L. 2002. Gelogical Features and origin of gold deposits occurring in the Baotou- Bayan Obo district, south_central Inner Mongolia, People's Republic of China. *Ore Geol. Rev.*, 20: 139~ 169.

PLYMATE T G, DANIEL C G. & CAVALERI, M.E. 1992. Structural state of the K_feldspar in the Butler Hill_Breadtray granite, St. Francois Mountain, Southeastern Missouri. *Can. Mineral.*, 30: 367~ 376.

RIBBE P H. 1983. Feldspar Mineralogy. Mineral. Soc. Am., Washington D.C.

SHEN Q H, ZHANG Y F, GAO J F & WANG P. 1990. Study on Archean metamorphic rocks in mid_southern Nei Mongol (Inner Mongolia) of China. *Chinese Acad. Geol. Sci., Inst. Geol. Bull.* 21: 156 (in Chinese).

TAN Y J, ZHANG W J. & SONG Y S. 2002. Mechanism and evolution of the migmatization in Wulashan rock group, Guyang, Inner Mongolia. *Geosci.*, 16(1): 31~ 36 (in Chinese).

TRUMBULL R B, HUA L, LEHRBERGER G, SATIR M, WIMBAUER, T. & MORTEANI, G. 1996. Granite_hosted gold deposits in the Anjiayinzi district of Inner Mongolia, People's Republic of China. *Econ. Geol.*, 91: 375~ 395.

WU S Q, JIANG Y, JIANG D M, LI S Z & YANG J K. 1995. Geologyof Hadamengou Pegmatite Gold Deposit, Inner Mongolia. Seismology Press, Beijing.

ZHANG H K, HU P & SHEN F X. 1997. Studies of information of mineralizing microcline and their significance in Wulashan gold deposit. *Earth. Sci.*, 22 (6): 1~ 5 (in Chinese).

ZHANG H T. 1991. *Granitoid magma series and gold metallogeny of the Baotou- Bayan Obo district* (Ph. D. thesis). Beijing: Chinese Acad. Geol. Sci (in Chinese).

ZHANG H T, SO C S & YUN S T. 1999. Regional geologic setting and metallogenesis of central Inner Mongolia, China: guides for exploration of mesothermal gold deposits. *Ore Geol Rev.*, 14: 129~ 146.

ZHANG L Q. 1989. Distribution and geologic features of gold deposits along the northern margin of the north China platform: *Geol Soc. Inner Mongolia Bull.*, 11: 1~ 6 (in Chinese).